Differential Multisite Phosphorylation of the Trehalose-6-phosphate Synthase Gene Family in *Arabidopsis thaliana*

A MASS SPECTROMETRY-BASED PROCESS FOR MULTIPARALLEL PEPTIDE LIBRARY PHOSPHORYLATION ANALYSIS*

Mirko Glinski and Wolfram Weckwerth‡

Multisite protein phosphorylation plays a fundamental role in metabolic regulation. To detect and quantify *in vitro* kinase phosphorylation activities, we developed a highly selective LC-MS/MS-based method using high resolution multiple reaction monitoring on a triple quadrupole mass spectrometer. This method eliminates the need for stable isotope labeling and enables multiparallel kinase target assays. Using these assays, we made the first observation of *in vitro* phosphorylation of different trehalose-6-phosphate synthase (TPS) isozymes. TPSs possess putative Ca^{2+}-independent, sucrose non-fermenting 1-related protein kinase 1 (SnRK1) phosphorylation sites. Sixteen synthetic peptides from six different *Arabidopsis thaliana* TPS isozymes containing the SnRK1 consensus recognition motif were phosphorylated simultaneously *in vitro*, and their phosphorylation dynamics were determined. We achieved absolute quantification of TPS peptide phosphorylation by tuning the mass spectrometer to the corresponding synthetic standard phosphopeptides. The selectivity of the mass spectrometer in the multiple reaction monitoring mode compensates for the low ionization efficiency of phosphopeptides in the presence of a complex matrix. Results are in close agreement with recent *in vivo* studies of TPS phosphorylation and regulation and reveal significant differences in the phosphorylation levels of different TPS members within the TPS gene family ranging over 3 orders of magnitude. Substituting EGTA for $CaCl_2$ in the reaction mixture reduced the formation of some of the phospho-TPS peptides drastically, indicating that Ca^{2+}-dependent kinases are active in the presence of Ca^{2+}-independent SnRKs. This agrees with the proposed overlap of the consensus motifs of these kinases and enables delineation between Ca^{2+}-independent and Ca^{2+}-dependent phosphorylation. Results demonstrate that multiparallel kinase target assays are sensitive enough to provide evidence for differential multisite phosphorylation of homologous TPS proteins and their highly conserved putative phosphorylation sites. *Molecular & Cellular Proteomics 4:1614–1625, 2005.*

Trehalose, a non-reducing disaccharide sugar composed of two glucose molecules, accumulates in a variety of organisms that have adapted to withstand diverse stress conditions such as salt, heat, or drought stress. The biosynthesis of trehalose occurs via a phosphorylated intermediate, trehalose 6-phosphate, with two steps catalyzed by the enzymes trehalose-6-phosphate synthase (TPS)[1] and trehalose-phosphate phosphatase. Higher plants can synthesize trehalose, but most do so at low levels (1–3); only in resurrection plants where trehalose works as an osmoprotectant during desiccation stress (4) is trehalose accumulated quantitatively. Although trehalose is widely distributed in nature and is known to play a role in carbohydrate storage and plant growth and development (5–7) little is known about its metabolism, and most of the regulation mechanisms are speculative.

Surprisingly the *Arabidopsis thaliana* genome contains numerous TPS and trehalose-phosphate phosphatase homologues (8). The expression of TPS genes occurs in various tissues and is controlled by numerous stimuli such as abiotic stress, nutritional stress, and circadian cycle (9, 10). The TPS gene At2g18700 is strongly induced during extended night conditions (low sugar levels) (9). Four other genes coding for TPS (At1g60140, At1g68020, At1g70290, and At1g23870) also show induction (9). Furthermore the *Arabidopsis TPS1* (At1g78580) mutant, disrupted in the trehalose-6-phosphate synthase gene, has a pronounced phenotype that could be interpreted as the consequence of glycolytic deregulation (8, 11). Recent transcriptomic analysis further revealed gene clusters that correlated with alterations in trehalose 6-phosphate levels (7). Among the genes identified, one was repressed by sucrose addition (7). This gene, *AtKIN11*, encodes a sucrose non-fermenting 1-related protein kinase (SnRK1) known to be involved in signal transduction affecting sugar utilization (13).

In a manner analogous to the biosynthetic key enzymes

From the Max Planck Institute of Molecular Plant Physiology, 14476 Potsdam-Golm, Germany

Received, May 11, 2005, and in revised form, July 8, 2005

Published, MCP Papers in Press, July 19, 2005, DOI 10.1074/mcp.M500134-MCP200

[1] The abbreviations used are: TPS, trehalose-6-phosphate synthase; CDPK, calcium-dependent protein kinase; FA, formic acid; FWHM, full width at half-maximum; LODs, limits of detection; MRM, multiple reaction monitoring; S/N, signal-to-noise; SnRK1, sucrose non-fermenting 1-related protein kinase 1; SPS, sucrose-phosphate synthase.

sucrose-phosphate synthase (SPS) and nitrate reductase, whose activity states are rapidly altered by protein kinase action in response to environmental changes and/or genetic perturbations present in mutant plants (14–17), the TPS enzyme also is thought to be regulated by reversible protein phosphorylation/dephosphorylation (18). The reversible phosphorylation of proteins is recognized as a common and important post-translational modification in eukaryotes. It alters the behavior of proteins and is well known to play a key regulatory role in cellular processes such as plant defense (19, 20), plant growth (21), energy metabolism (22), and stress responses (23, 24). It is estimated that ~30% of all proteins expressed in eukaryotic cells exist in phosphorylated forms at any given time (25–27). In *Arabidopsis*, the regulation of these highly dynamic phosphorylation states is achieved by ~1100 protein kinases and 100–200 protein phosphatases (28, 29).

The Ca^{2+}-independent SnRK1 subgroup is involved in signaling pathways controlling fundamental cellular processes. SnRK1 is the closest plant homologue of yeast sucrose nonfermenting-1 protein kinase and of the AMP-activated protein kinase in animals. The identification of SnRK1 substrates like SPS and nitrate reductase (14, 30–32) demonstrated the roles of these kinases in regulating biosynthetic pathways such as sucrose synthesis and nitrogen assimilation. Furthermore SnRK1 is involved in plant growth (33) and was shown to play a role in plant development (34). In *Arabidopsis* there are three known SnRK1s (35), one of which is thought to be subject to regulation by glucose 6-phosphate (36). Moreover *Arabidopsis* TPSs possess putative SnRK1 phosphorylation sites.

MS has become the method of choice for profiling post-translational modifications, in particular reversible phosphorylation. Such applications help us gain insight into protein regulation at the cellular level. For phosphopeptide analysis, characteristic marker ions at *m/z* 63 (PO_2^-) and/or 79 (PO_3^-) are used in precursor ion scan mode (37–39). Furthermore phosphopeptide-specific neutral losses of H_3PO_4 (98 Da) or HPO_3 (80 Da) are utilized for identification in neutral loss MS experiments (40, 41). We recently developed a robust non-targeted and stable isotope-based method for the routine quantification of phosphorylation at specific sites (42). The method allows the simultaneous identification and quantification of a multitude of *in vitro* phosphorylated synthetic peptides. We have observed clear differences in the phosphorylation states of *Arabidopsis* wild-type and mutant plant SPS (42). Although it is a very homologous system using substrates similar to those used in sucrose biosynthesis, no investigations on the regulation of TPS isoforms via post-translational phosphorylation have been reported.

As a complement to the non-targeted approach, we developed a stable isotope-free method for the highly selective detection and absolute quantification of target phosphopeptides using LC coupled to tandem mass spectrometry in MRM mode. Although phosphopeptides are generally not observed as intense peaks due to ionic suppression, especially in the presence of non-phosphorylated peptides (43, 44), our MRM-based method allows a significant enhancement of signal-to-noise (S/N) ratios in phosphopeptide analysis and compensates for the low ionization efficiency of phosphopeptides in positive ionization mode by the high selectivity of the mass spectrometer using MRM. This enabled us to look at TPS isoform phosphorylation states in *Arabidopsis* for the first time

EXPERIMENTAL PROCEDURES

Chemicals and Reagents—Synthetic (phospho)peptides were purchased from peptides&elephants GmbH (Nuthetal, Germany). The peptide sequences were deduced from six *Arabidopsis* TPS isozymes (At1g23870, At1g60140, At1g68020, At1g70290, At1g78580, and At2g18700). Microcystin was from Cyano Biotech GmbH (Berlin, Germany). Acetonitrile (LC-MS grade) was purchased from J. T. Baker Inc. Distilled water was purified "in-house" using a Milli-Q system (Millipore, Billerica, MA). All other chemicals and reagents were obtained from Sigma and were of the highest purity commercially available.

Extraction of Protein Kinases from Arabidopsis Leaves—Frozen *Arabidopsis* wild-type leaf tissue (usually 300 mg fresh weight) was ground in a chilled mortar. After addition of 400 μl of extraction buffer containing 50 mM Tris-HCl, pH 7.5, 20% (v/v) glycerol, 5 mM dithiothreitol, 1 mM benzamidine, 0.3 μM microcystin, 60 mM sodium fluoride, 2 mM 4-(2-aminoethyl)benzenesulfonyl fluoride, 100 μM bestatin, 20 μM pepstatin A, 20 μM leupeptin, 30 μM (2*S*,3*S*)-3-(*N*-{(*S*)-1-[*N*-(4-guanidinobutyl)carbamoyl]3-methylbutyl}carbamoyl)oxirane-2-carboxylic acid, and 5 mM 1,10-phenanthroline, the crude extract was placed on ice for 20 min and was then centrifuged at 15,000 × *g* for 5 min. The supernatant was subsequently desalted on a Sephadex G-25 column (1 × 5 cm) previously equilibrated with extraction buffer containing no glycerol. The volume of eluent from the Sephadex G-25 column was 1 ml.

Determination of Protein Content—Protein concentrations were determined via the dye-binding method of Bradford as described previously (45) using bovine serum albumin as a standard. Each measurement was made in triplicate, and the mean values were used. 300 mg of *Arabidopsis* wild-type leaf tissue (fresh weight) used in each assay yielded 3 mg of total protein.

In Vitro Kinase Activity Assay—Typically each 100-μl kinase assay reaction mixture contained 50 μl of desalted *Arabidopsis* crude extract, 25 μM synthetic TPS peptide, 10 mM $MgCl_2$, 5 mM ATP, and 1 mM $CaCl_2$. Where specified, $CaCl_2$ was replaced by 4 mM EGTA for the Ca^{2+}-independent kinase activity assay. The reaction was initiated by the addition of desalted *Arabidopsis* crude extract. Following a 15-min incubation at 25 °C, the reaction was stopped by adding 500 μl of ice-cold EtOH. After standing on ice for 20 min, the mixture was centrifuged at 15,000 × *g* for 2 min. The supernatant was then evaporated in a centrifugal vacuum system (SpeedVac), reconstituted in 10 μl of 0.1% formic acid (FA) in water, and finally injected into the LC-MS/MS system.

Preparation of Calibration Curves with Phosphorylated TPS Peptide Standards—1 mM stock solutions of synthetic phosphorylated TPS peptides were prepared in 50 mM Tris-HCl, pH 7.5. These stock solutions were diluted further to make working solutions and stored at −20 °C. Aliquots of working solutions were spiked into kinase activity assay reaction mixtures instead of their non-phosphorylated counterparts. Following incubation and sample preparation as described above, the reconstituted TPS phosphopeptides were used for the calibration curves. The construction of calibration curves with phosphopeptide standards was done on a daily basis.

Liquid Chromatography—The HPLC system consisted of a Surveyor autosampler and Surveyor MS pump with an integrated degas-

ser (ThermoFinnigan, San Jose, CA). The chromatographic separation of phosphopeptides was performed on a 100 × 1-mm, 3-μm, Luna C_{18} (2) column (Phenomenex, Aschaffenburg, Germany) that was directly interfaced to the ESI source of the mass spectrometer. Mobile phase A (0.1% FA in Milli-Q water (v/v)) and mobile phase B (0.1% FA in acetonitrile (v/v)) were used for elution. The gradient transitioned from 0 to 40% phase B during the first 25 min followed by 40–80% phase B over a 1-min period. It was held for 10 min at 80% phase B and then transitioned back to 0% phase B over a 2-min period with a flow rate of 40 μl/min. Re-equilibration was performed at 0% B for 15 min with a flow rate of 60 μl/min. The injection volumes were 10 μl.

Mass Spectrometry—Mass spectrometry was performed on a TSQ Quantum Discovery MAX mass spectrometer (ThermoFinnigan) equipped with an Ion Max ESI source with a 34-gauge metal needle operated under Xcalibur™ software (version 1.4 SR1, ThermoFinnigan) in the positive ion mode. The collision cell was pressurized with argon. Mass spectrometric detection of positively charged phosphopeptides was achieved with MRM for which the following tune parameters were set: sheath gas pressure of 30 arbitrary units; spray voltage set to 3.7 kV; temperature of the heated transfer capillary, 270 °C; collision gas pressure, 1.5 millitorrs. The scan width for all MRMs was 0.7 mass units. The resolution for Q1 was 0.3 mass units; the resolution for Q3 was set to 0.7 mass units. The collision energies used for the recorded transitions are shown in Table I. The dwell time per transition was 50 ms. To demonstrate the impact of the Q1 resolution setting on peak purity and selectivity of the detection the mass spectrometer was set at Q1 resolutions of 0.7, 0.5, and 0.3 Da full width at half-maximum (FHWM), respectively, and at a Q3 resolution of 0.7 Da FHWM.

The mass spectrometer was tuned to its optimum sensitivity by infusing solutions containing 10 pmol/μl of each phosphorylated TPS standard peptide in H_2O/acetonitrile (50:50, v/v) containing 0.1% FA at a constant flow rate of 40 μl/min. For that, the phosphorylated TPS peptides were first characterized by MS and then MS/MS to ascertain their precursor ions and to select product ions for use in MRM mode. The dominant peaks in the full-scan spectra were used for collision-induced dissociation to produce characteristic fragment ions for each phosphopeptide. To enhance sensitivity, we performed subsequent optimization of the two most abundant MRM transitions for each phosphopeptide and selected the corresponding precursor and product ion pairs (Table I) for quantitative analysis. For the mass spectrometric detection of TPS phosphopeptides using full-scan mode, the mass range was set to *m/z* 300–900, and the resolution for Q3 was 0.7 mass units.

For the identification of phosphorylation sites MS^3 spectra were recorded on an LTQ linear ion trap mass spectrometer (ThermoFinnigan). The isolation width was 2.0 mass units, the activation was set to 0.25, and the activation time was 30 ms. TPS phosphopeptides and phosphorylation sites were identified by automatic data-dependent acquisition consisting of a MS^2 of the known precursor ions (TPS phosphopeptides) and a subsequent MS^3 scan on the neutral loss fragments (m/z = 49, H_3PO_4 for the doubly charged ions).

Quantification—For the quantification of TPS phosphopeptides formed in the *in vitro* kinase assay, the two most abundant MRM transitions for each phosphopeptide (Table I) were used based on their observed fragmentation behavior. Subsequent processing of product ion chromatograms and peak integration was performed using the ICIS algorithm in LCquan™ 2.0 (Xcalibur software, version 1.4 SR1, ThermoFinnigan). Absolute amounts of phosphopeptides were calculated from the slope of peak area ratios of the *in vitro* formed phosphopeptides and calibration standards using the least square linear regression (weighting factor 1/concentration).

RESULTS

Initial Method Demonstration—To demonstrate the suitability of our MRM-based approach for the specific and accurate identification and quantification of phosphorylation levels at targeted TPS phosphorylation sites, the *in vitro* formation of multiply phosphorylated TPS peptide forms (and the conversion of target TPS phosphopeptides to multiply phosphorylated TPS peptides, respectively) catalyzed by other kinase families had to be ruled out. For that purpose, TPS standard peptides were simultaneously incubated *in vitro* and assayed for kinase activity as described above (see "Experimental Procedures"). In an analogous experiment, the TPS standard peptides in the reaction mixture were substituted by their phosphorylated TPS counterparts. Mass spectrometric full-scan detection of the reaction products formed in the presence and absence of ATP unambiguously revealed the exclusive formation of singly phosphorylated TPS peptides. No multiply phosphorylated TPS peptides were formed under the *in vitro* kinase assay conditions.

Selectivity of Detection—The selective detection and identification of target TPS phosphopeptides formed in the multiparallel *in vitro* kinase assay were achieved by collision-induced dissociation, which allows the MS/MS system to be operated in the positive ionization MRM mode. By applying the optimum tuning parameters for each individual selected precursor/product ion transition, the two most abundant fragments (product ions) of each TPS phosphopeptide were used for quantification, thus verifying the selectivity of the method. As a result, identical amounts of phosphorylated analytes were obtained using calibration curves with both product ions. The phosphopeptide level ratios determined from the two MRM transitions were close to unity and proved stable for the calibration standards and the plant samples indicating that the approach was selective for the detection and quantification of TPS phosphopeptides formed in the multiparallel *in vitro* kinase activity assay.

A comparison of the MRM-based LC-MS/MS strategy with full-scan detection (in the mass range *m/z* 300–900) is shown in Fig. 1. As can be seen, the S/N ratios for the *in vitro* formed TPS phosphopeptides detected in MRM mode are considerably higher than those observed using full-scan detection, demonstrating the high selectivity and specificity of the MRM-based method (Fig. 1 and Table I). The S/N gains ranged from 3.2 to 8.0. In Fig. 1, *B* and *C*, the extracted ion chromatograms for the phosphorylated TPS peptides 1 and 8 are shown for the mass spectrometric detection using the MRM mode and full-scan detection, respectively.

Reversed-phase HPLC further enhanced the signals of the phosphopeptides, thus reducing ion suppression by matrix interference (46). Retention times of *in vitro* formed phosphorylated TPS peptides agreed within ±2% with the retention times for the reference standards and served as important criteria for unambiguous identification.

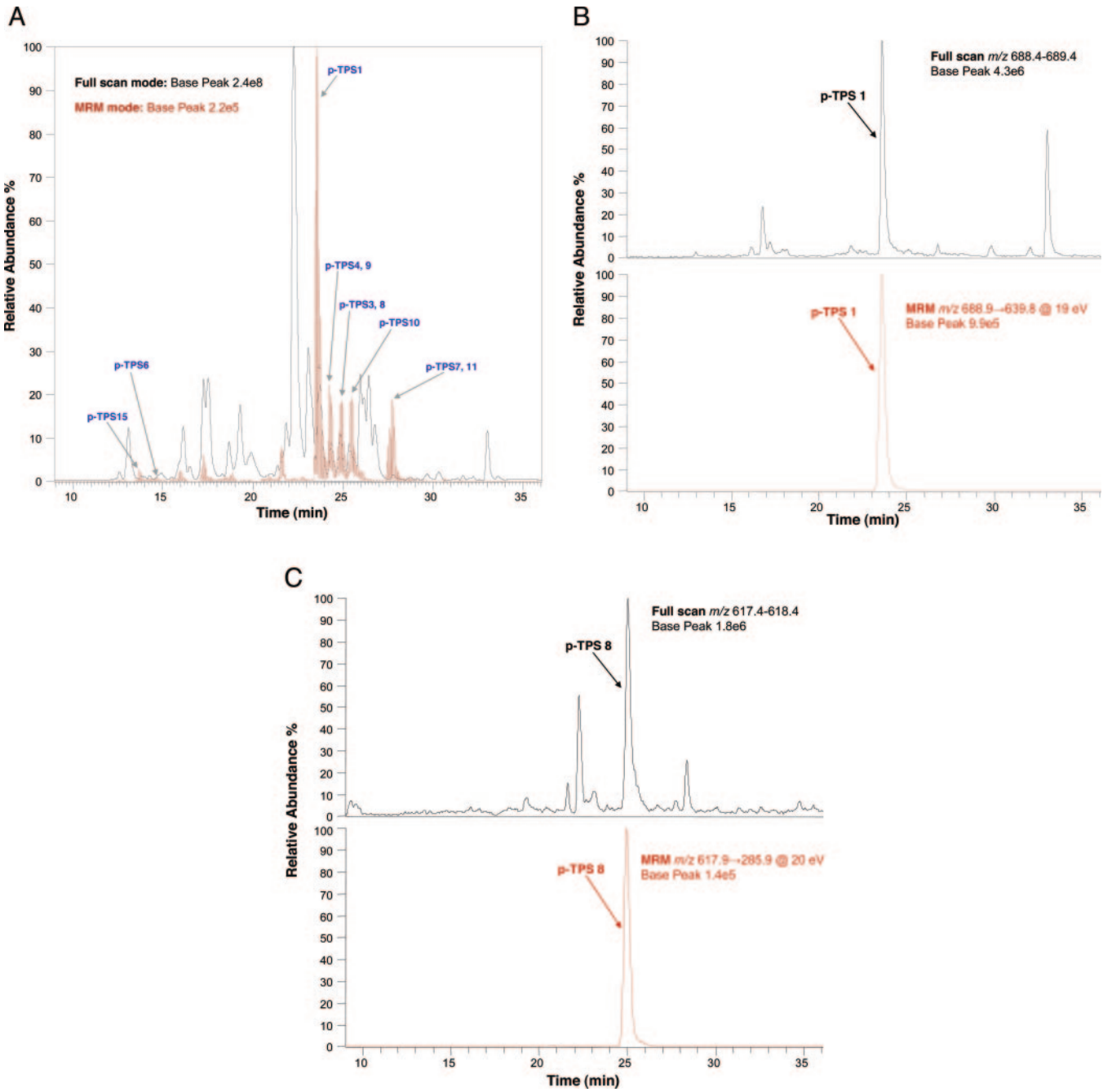

FIG. 1. *A*, reversed-phase separation of *in vitro* phosphorylated TPS peptides based on mass spectrometric detection using full-scan mode in the mass range *m/z* 300–900 (base peak chromatogram) and MRM. *B*, extracted ion chromatograms for the phosphorylated TPS peptide 1 (*m/z* 688.9, +2) detected in full-scan mode and MRM mode. *C*, extracted ion chromatograms for the phosphorylated TPS peptide 8 (*m/z* 617.9, +2) detected in full-scan mode and MRM mode.

Enhanced Q1 Resolution and Peak Purity in MRM—To test and compare the sensitivity and selectivity of the mass spectrometer under typical conditions for quantitative investigations, the TPS phosphopeptides were injected on-column and analyzed in MRM mode using three different resolution settings for Q1 (0.7, 0.5, and 0.3 Da FHWM) and fixed Q3 resolution (0.7 Da FHWM). As an example, Fig. 2 shows the MRM chromatograms of phospho-TPS peptide 8 obtained after chromatographic separation. As can be seen, enhanced resolution (Q1 = 0.3 Da FHWM, Q3 = 0.7 Da FHWM) is a valuable tool to eliminate interfering substances having the same nominal mass as the target phosphopeptide and background noise. Under enhanced resolution, the peak area of the target phosphopeptide was ~5-fold lower than that ob-

TABLE I

List of TPS target peptides used in this study, their behavior in the in vitro kinase activity assay, and mass spectrometric and chromatographic parameters for the quantification of TPS phosphopeptides

The quantitative data are composed of the measures of quantification for the two most abundant MRM transitions. The phosphorylated serine/threonine residue is in bold. N.D. indicates not detectable/quantifiable after *in vitro* kinase activity assay.

TPS isozyme	TPS peptide sequence	TPS peptide no.	Precursor ion (*m/z*)	Product ions (*m/z*)	Collision energy	Elution time	S/N ratio MRM	S/N ratio full-scan mode	S/N gain	LOD in MRM	*In vitro* phospho-rylation	Dependence on Ca^{2+}	Consensus motif[a]
					eV	*min*				*fmol*			
At2g18700	YFGRTV**S**IKIL	1	688.9	639.8 906.2	19 31	23.6	77,400	10,670	7.2	1,100	Yes	+	Preferred
	TLDKRP**S**DDLI	2	676.8	186.9 627.6	35 20	18.9	N.D.	N.D.		40	No		Preferred
At1g70290	TLPRVM**T**VPGI	3	632.3	285.9 880.3	17 20	24.9	20,370	2,700	7.5	100	Yes	−	Preferred
	HMGRLE**S**VLSL	4	661.3	446.5 612.2	24 17	24.3	8,670	1,720	5.0	50	Yes	+	Preferred
	ALKMSE**T**EKQL	5	679.3	128.8 630.2	37 18	17.1	N.D.	N.D.		130	No	−	Less preferred
	SLKPSS**S**HTQV	6	625.8	128.7 567.4	25 18	14.3	210	65	3.2	170	Yes	−	Less preferred
	DIFKGI**S**LKLI	7	663.9	128.8 614.7	29 19	27.6	11,520	1,920	6.0	20	Yes	+	Preferred
At1g23870	DIFKGI**S**LKLI	7	663.9	128.8 614.7	32 19	27.6	11,520	1,920	6.0	20	Yes	+	Preferred
	ALPRVM**T**VPGI	8	617.9	285.9 850.3	16 20	25.0	27,280	4,330	6.3	190	Yes	−	Preferred
	HMGRLE**S**VLNL	9	674.8	609.3 625.7	20 19	24.3	16,200	3,240	5.0	50	Yes	+	Preferred
At1g60140	HMGRLE**S**VLNL	9	674.8	609.3 625.7	20 19	24.3	16,200	3,240	5.0	50	Yes	+	Preferred
	YLPRVM**T**VPGI	10	663.3	285.8 942.4	19 22	25.5	21,780	2,730	8.0	50	Yes	−	Preferred
	DIFKGL**S**LKIL	11	663.9	128.8 614.7	32 19	27.7	11,520	1,920	6.0	20	Yes	+	Preferred
	SIVKDP**S**AEVI	12	619.3	172.8 909.3	25 21	20.6	N.D.	N.D.		90	No		Preferred
At1g68020	SFKCVP**T**FLPL	13	666.3	228.8 1,005.4	19 17	28.7	N.D.	N.D.		40	No		Less preferred
	DIFKGI**T**LKLL	14	670.9	128.8 621.7	31 17	27.6	N.D.	N.D.		40	No		Preferred
	SIDKRP**S**SKSI	15	649.3	172.8 600.2	35 20	13.7	2,920	650	4.5	30	Yes	+	Preferred
At1g78580	CLKEYN**S**KMKV	16	711.8	128.8 662.7	34 20	16.0	N.D.	N.D.		850	No		Less preferred

[a] According to Halford and Hardie (47).

served at Q1 resolution 0.7 Da FHWM (Fig. 2). The S/N ratio, however, only decreased by a factor of 2. The ratio of S/N and peak area (S/N:peak area) was used as an indicator of peak purity. An increasing ratio signifies higher peak purity. Increasing the resolution of Q1 from 0.7 to 0.3 Da FHWM resulted in an increase of (S/N:peak area) from 0.001 to 0.0024. Thus, the peak purity significantly increased under enhanced resolution making the detection considerably more selective. Changing Q3 resolution from 0.7 to 0.5 Da FHWM under enhanced resolution did not further improve the selectivity of the measurement (data not shown). This indicates the predominant role of the Q1 resolution setting (rather than Q3) in peak purity and therefore selectivity of the mass spectrometric detection in MRM mode. To avoid interference peaks that can hamper the quantitative analysis of phosphorylation levels and therefore to achieve high peak purity, the mass spectrometer was always operated under enhanced resolution.

Recovery of in Vitro Phosphorylated TPS Peptides—Determining individual recoveries after sample preparation is indispensable when quantifying phosphopeptide levels. To look at recoveries, phosphorylated TPS standard peptides of known concentrations were simultaneously incubated *in vitro* and assayed for kinase activity as described above (see "Experimental Procedures"). In a control experiment, the phospho-TPS standard peptides were omitted in the reaction mixture and added after incubation and sample preparation. After LC-MS/MS analyses using MRM, the recoveries of phosphorylated TPS peptides were calculated from the ratio of peak areas of phosphorylated TPS peptide standards in the control samples and in incubated samples. The resulting TPS phosphopeptide recovery rates varied from 50 to 95%. However, differences in rates were compensated for by including matrix effects and all steps of sample preparation into the calibration curves. Therefore, no correction factors for the compensation

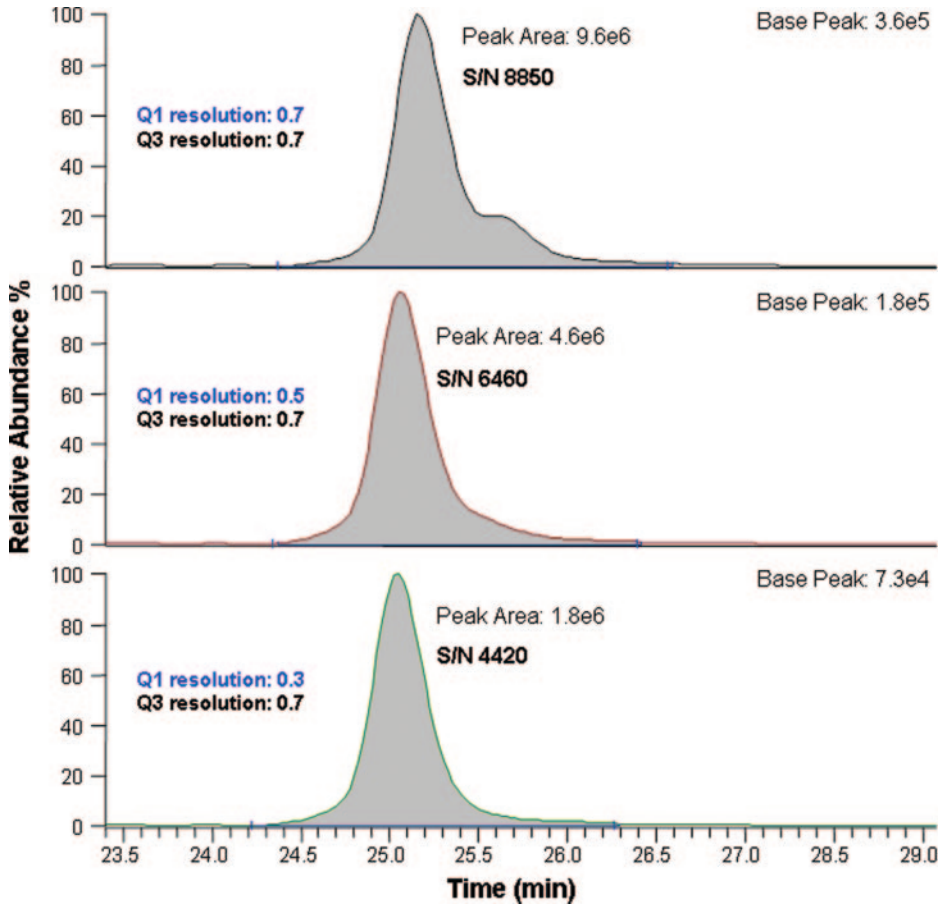

FIG. 2. **MRM chromatograms of 5 pmol of TPS phosphopeptide 8 obtained at three different Q1 resolution settings.**

of differential recovery of phosphopeptides are needed. This makes the *in vitro* kinase assay independent from individual recovery levels of phosphopeptides, excluding false quantifications caused by non-reproducible recovery levels.

Linearity of Quantification—To quantify phosphorylation reliably, method linearity validation is essential. To this end, calibration curves with synthetic standard TPS phosphopeptides were constructed, and the linearity of the method from 0.5–500 pmol for all TPS phosphopeptides was investigated. Each measurement was done in triplicate. Using the least square linear regression (weighting factor 1/concentration) the coefficients of regression (r^2) were determined to be 0.9883–0.9964 confirming a linear dependence of the amounts of TPS phosphopeptides and peak areas of the corresponding MRM transition. In Fig. 3 the calibration curves for two phosphorylated TPS peptides, p-TPS1 and p-TPS8, are depicted as examples.

Comparison of Multiparallel and Single Incubation Peptide Phosphorylation Assays—A significant improvement of the mass spectrometric analysis of peptide phosphorylation over classical radioactive incorporation studies is the possibility of incubating a multitude of substrates simultaneously. However, this may lead to artificial competition between individual TPS peptides in the assay. Therefore, each TPS peptide was incubated alone, and the amount of the corresponding phosphopeptide formed was compared with the amount formed in multiparallel incubations. As a result, no significant reduction of phosphopeptide formation was observed in multiparallel incubations (data not shown). Hence a disturbing competitive effect caused by the multitude of individual substrate TPS peptides was ruled out for the *in vitro* kinase activity assay.

In Vitro Phosphorylation of TPS Peptides: Ca^{2+} Dependence and Independence—After establishing the described MS-based kinase assay system, we started to investigate the *in vitro* phosphorylation of TPS homologues in *Arabidopsis*. Beyond verifying TPS protein phosphorylation, three other questions have been central. (i) Based on transcriptomic analyses a Ca^{2+}-independent kinase is known to cluster with trehalose accumulation (see the Introduction). Consequently we investigated the Ca^{2+} dependence of protein phosphorylation. (ii) We analyzed further whether the different TPS isozymes in *Arabidopsis* are differentially phosphorylated and (iii) to what extent multisite phosphorylation occurs for different TPS protein isozymes. To address these questions we first needed to determine whether the method is sensitive and selective enough to see differences among the phosphorylation levels of substrate TPS peptides.

The limits of detection (LODs) for all TPS phosphopeptides

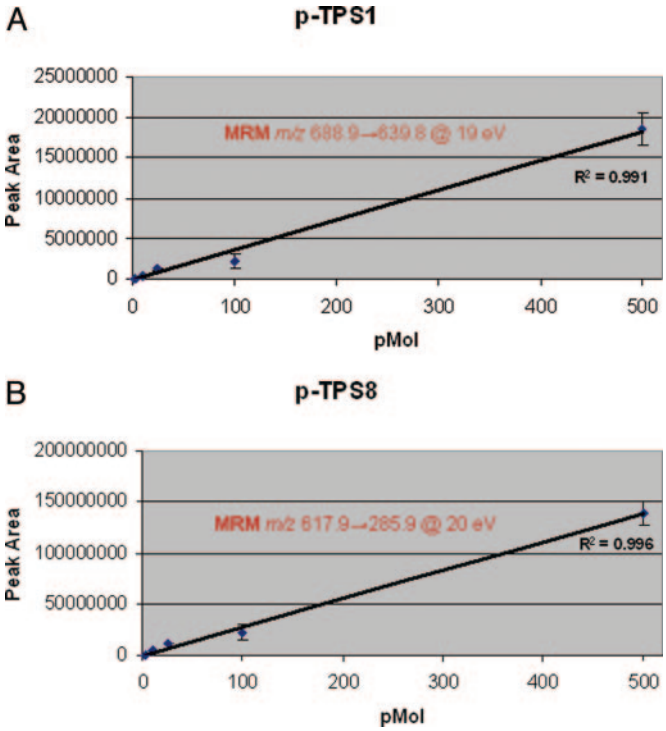

FIG. 3. **Calibration curves for the phosphorylated TPS peptide 1 (*A*) and for the phosphorylated TPS peptide 8 (*B*).** *Error bars* indicate ±S.D. of triplicate analysis.

B

TPS Peptide	Sequence	Residues	TPS Isoform
1	YFGRTVSIKIL	283-293	At2g18700
2	TLDKRPSDDLI	599-609	At2g18700
3	TLPRVMTVPGI	26-36	At1g70290
4	HMGRLESVLSL	305-315	At1g70290
5	ALKMSETEKQL	504-514	At1g70290
6	SLKPSSSHTQV	840-850	At1g70290
7	DIFKGISLKLI	344-354 342-352	At1g70290 At1g23870
8	ALPRVMTVPGI	26-36	At1g23870
9	HMGRLESVLNL	307-317 307-317	At1g23870 At1g60140
10	YLPRVMTVPGI	26-36	At1g60140
11	DIFKGLSLKIL	344-354	At1g60140
12	SIVKDPSAEVI	607-617	At1g60140
13	SFKCVPTFLPL	137-147	At1g68020
14	DIFKGITLKLL	354-364	At1g68020
15	SIDKRPSSKSI	618-628	At1g68020
16	CLKEYNSKMKV	246-256	At1g78580

FIG. 4. **Consensus sequence and alternatives for recognition by members of the SnRK1 subfamily (*A*) and sequences of TPS substrate peptides used in the *in vitro* kinase assay (*B*).** The requisite residues are the target serine/threonine (in *green*), hydrophobic residues at +4 and −5 with respect to the serine/threonine (in *blue*), and a basic residue at −3 (in *red*) or (less preferably) at −4 (in *pink*). *X* is any residue. The peptide sequences were obtained by alignment of the consensus sequence and alternatives with six different TPS isozymes from *Arabidopsis*. The residue *numbers* specify the position of each peptide sequence on the corresponding TPS isozymes (*Arabidopsis* gene identification codes are shown). All sequences are from the Munich Information Centre for Protein Sequences (MIPS) database.

were determined by spiking matrix (*Arabidopsis* crude extract) with phosphorylated TPS standard peptides of known concentration and subsequently subjecting the mixture to LC-MS/MS analysis with MRM as described above. The S/N ratios were calculated from the ratio between analyte peak signal to base-line noise. The estimated LODs at 3 times S/N are shown in Table I.

Target peptide sequences were obtained by aligning the sequences of six different *Arabidopsis* TPS isozymes with the consensus sequence and alternatives for recognition of the SnRK1 subfamily (Fig. 4*A*) (47). The corresponding TPS genes At2g18700, At1g60140, At1g68020, At1g70290, and At1g23870 show (strong) induction under extended night conditions (9), and the *Arabidopsis TPS1* (At1g78580) mutant, disrupted in the trehalose-6-phosphate synthase gene, exhibits a pronounced phenotype (8, 11).

The residues within the TPS substrate peptides required for recognition by SnRK1s are highlighted in Fig. 4*B*. As can be seen, due to partial sequence identity of TPS isozymes, TPS peptides 7 and 9 represent internal sequences of two different TPS isozymes at the same time. To test whether the TPS peptides are targeted by SnRK1s, *in vitro* kinase activity assays with extracts from *Arabidopsis* wild-type leaves were carried out as described under "Experimental Procedures." For the analyses, different lots of plants harvested in the middle of the light period of their growing cycle were analyzed. In subsequent mass spectrometric analyses, selective detection and absolute quantification of phosphorylated products were achieved in positive ionization mode with MRM for the two most abundant transition of each TPS phosphopeptide (see Table I). Despite differences in sensitivity, the second most abundant MRM transition for each TPS peptide was recorded as a further control of compound identity.

In a control experiment, ATP was omitted in the reaction mixture. Here apparent *in vitro* phosphorylation of TPS peptides most likely resulted from remaining endogenous (kinase-bound) ATP in the desalted crude extract. This "background phosphorylation" was subtracted from the amounts of phosphopeptides formed in the kinase activity assay upon addition of exogenous ATP. The absolute quantities of TPS phosphopeptides formed (taking into account the combined quantitative data obtained from the two most abundant MRM transitions for each TPS phosphopeptide) corresponding to

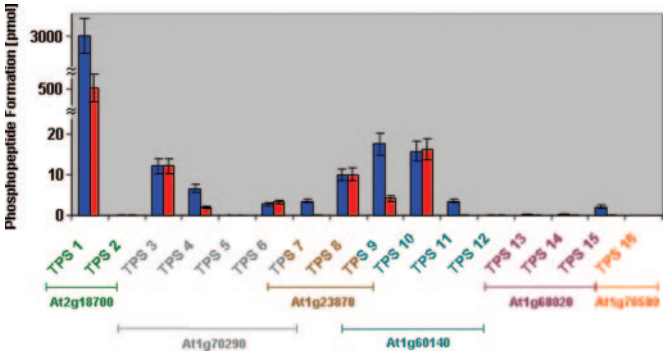

FIG. 5. **Absolute quantification of kinase activities in *Arabidopsis* wild-type plants harvested in the middle of the light period of their growing cycle.** In the multiparallel kinase activity assay, 16 TPS target peptides served as potential substrates for Ca^{2+}-independent SnRK1 subgroup kinases. For six target peptides, no corresponding phosphorylated peptides were observed. The *Arabidopsis* gene identification codes of the corresponding TPS isozymes are indicated. The *blue bars* refer to incubation with $CaCl_2$. The *red bars* refer to incubations where $CaCl_2$ was replaced with 4 mM EGTA. *Error bars* indicate ±S.D. of triplicate analysis.

extracted *in vitro* kinase activities are shown in Fig. 5. Reproducibility of absolute quantification of several independent replicates was ~20% mean coefficient of variance. This level of precision is useful for most biological problems.

As is illustrated in Fig. 5, within the series of the 16 TPS substrates used in this study, the levels of peptide phosphorylation were drastically different. The formation of the corresponding TPS phosphopeptides spanned 3 orders of magnitude. In this regard, TPS peptide 1 (corresponding to TPS isozyme At2g18700) is obviously an exceptionally highly preferred kinase target. The amount of the corresponding phosphopeptide was determined to be about 3 nmol. For the correct quantification of such a high amount of phosphopeptide, the samples were diluted before LC-MS/MS analysis to suit the working range. This circumvented saturation of the MS detector and hence an underestimate of product formation. TPS peptides 5 (TPS isozyme At1g70290), 6 (At1g70290) 13 (At1g68020), and 16 (At1g78580) exhibiting the less preferred consensus motif for SnRK1s have the requisite basic residue in position −4 with respect to the target serine/threonine. Fig. 5 and Table I show that three of these peptides (5, 13, and 16) were indeed either not phosphorylated *in vitro*, or their corresponding phosphopeptides were not detectable/quantifiable with our method. Only peptide 6 was phosphorylated and only to a low extent.

Furthermore the *in vitro* phosphorylation of six TPS peptides (1, 4, 7, 9, 11, and 15) corresponding to the TPS isozymes At2g18700, At1g70290, At1g23870, At1g60140, and At1g68020 exhibited a (partially) strong Ca^{2+} dependence (Fig. 5 and Table I). When $CaCl_2$ in the reaction mixture was replaced with 4 mM EGTA, the formation of the corresponding phospho-TPS peptides was significantly reduced. This indicates that Ca^{2+}-dependent kinases in the crude extract also recognize these peptides as substrates. As can be seen, Ca^{2+}-dependent kinases represent the dominant phosphorylating activity; Ca^{2+}-independent kinase(s) phosphorylated a smaller portion of TPS peptides. In this context, the Ca^{2+} dependence of phosphopeptide formation is particularly pronounced for TPS peptides 7, 11, and 15 (TPS isozymes At1g70290, At1g23870, At1g60140, and At1g68020) where the formation of the corresponding phosphopeptides is reduced by 100% in the absence of $CaCl_2$.

Identification of Phosphorylation Sites—The determination of the phosphorylated sites of the TPS peptides was done by the generation of neutral loss-driven MS^3 spectra using a linear ion trap mass spectrometer (see "Experimental Procedures"). As a result of MS^3 sufficient peptide backbone fragmentation of the TPS phosphopeptides was achieved to identify the correct phosphorylation sites. It could be shown that the full MS^3 spectra of standard TPS phosphopeptides were identical to the full MS^3 spectra obtained from *in vitro* formed TPS phosphopeptides thus providing evidence that the phosphorylated site of TPS peptides phosphorylated in the *in vitro* kinase assay was indeed the SnRK1 phosphorylation site (Fig. 6).

DISCUSSION

Using the novel approach described here, we were able to absolutely quantify peptide phosphorylation levels in biological samples without the need for stable isotope labeling. This approach combines multiparallel *in vitro* phosphorylation of putative kinase target peptides and fast, highly selective and sensitive LC-MS/MS analyses of the reaction products in MRM mode. The coupling of LC with MS/MS detection in the MRM mode has high specificity because only ions derived from the analytes of interest are monitored. In this context, the selectivity is significantly enhanced by the settings of the peak widths for ions passed by the Q1 (0.3 mass resolution units) and Q3 (0.7 mass resolution units) mass analyzers and the narrow scan range (0.7 mass units) for each MRM transition.

Although absolute signal intensity and peak area obtained with this enhanced resolution were 5-fold lower compared with Q1 and Q3 0.7 Da FWHM (Fig. 2), the selectivity of detection was greatly increased. This is a clear advantage in eliminating interfering matrix compounds. At enhanced resolution, only the desired precursor ions pass through Q1. The resulting MRM mass chromatograms contain peaks of higher purity due to the exclusion of co-eluting ions that have the same nominal mass as the target peptides and that yield product ions of the nominal same mass as the target peptides. Thus, the resolution setting of Q1 has a much higher impact on peak purity than that of Q3.

Using this strategy, we have provided the first evidence for *in vitro* phosphorylation of TPS gene family peptides. This data makes possible the selective screening of upstream kinases potentially involved in TPS regulation via phosphorylation *in vivo*. The targeted approach described here comple-

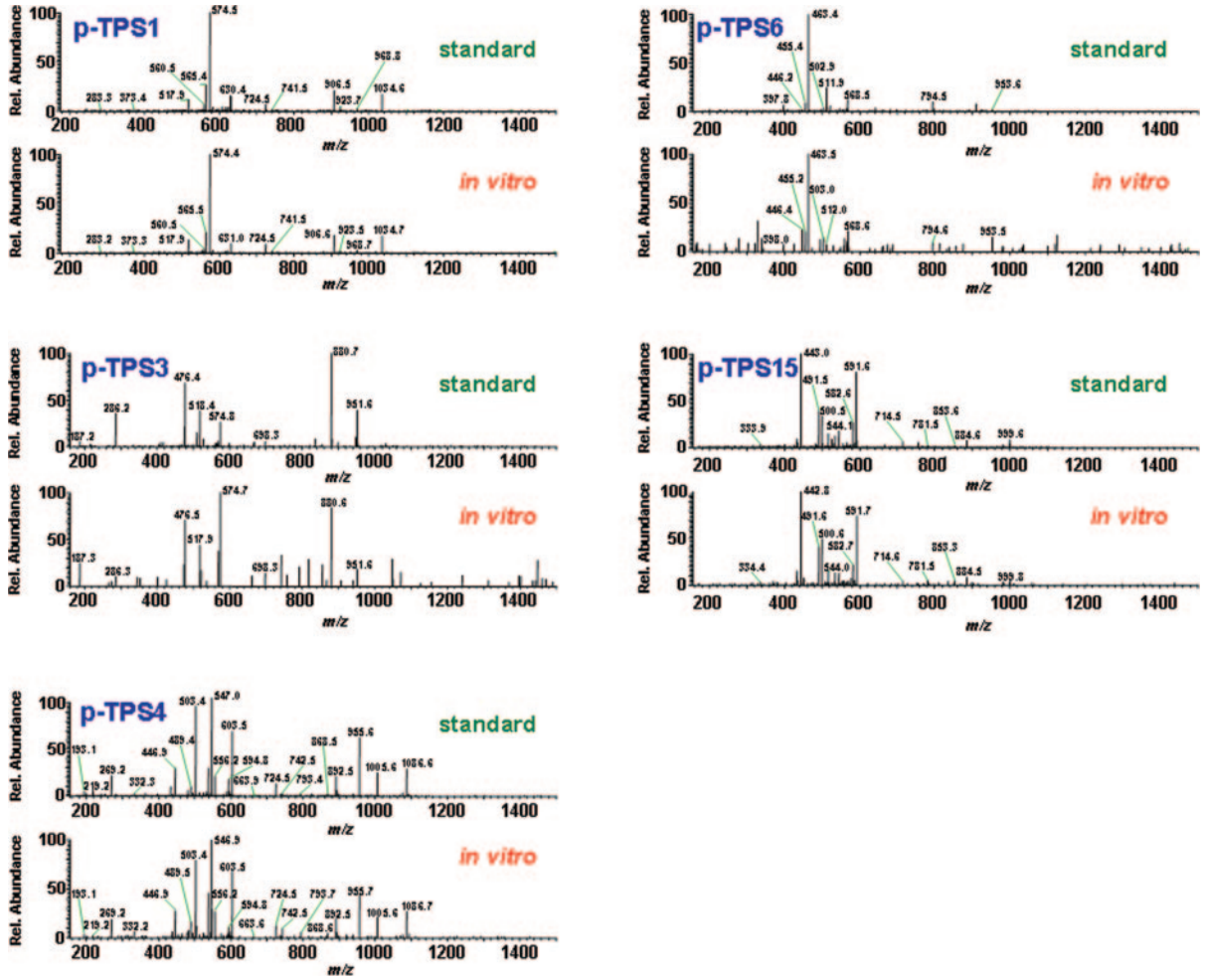

FIG. 6. **Comparison of MS^3 spectra obtained from synthetic standard phospho-TPS peptides 1, 3, 4, 6, and 15 and their corresponding TPS phosphopeptides formed in the *in vitro* kinase activity assay.** *Rel.*, relative.

ments our recently developed non-targeted stable isotope labeling strategy for the relative quantification of phosphopeptides in different biological samples. The use of the MRM mode for the mass spectrometric analysis allows highly selective detection and quantification of target phosphopeptides, whereas differential labeling allows identification of novel phosphorylation sites via *de novo* sequencing. The low ionization efficiency of phosphopeptides in positive ionization mode often hampers mass spectrometric analysis of phosphopeptides, resulting in rather low signal intensities, especially in the presence of non-phosphorylated peptides. A major advantage of our LC-MS/MS-based strategy is that it overcomes this drawback by the high selectivity of the triple quadrupole instrument in the MRM mode.

Studies on the recovery of phosphorylated reaction products of *in vitro* incubations have revealed enormous differences among TPS phosphopeptides, making quantification of phosphorylation levels a difficult task. Low phosphopeptide recoveries are probably due to nonspecific binding of *in vitro* formed phosphopeptides to reaction mixture proteins. The addition of EtOH to the reaction mixture results in the precipitation of proteins thus terminating the reaction. However, protein-bound TPS phosphopeptides co-precipitate, thereby reducing individual recoveries. Therefore, to absolutely quantify phosphopeptides the construction of calibration curves including the individual recoveries of TPS phosphopeptides is essential. We achieved this by substituting phosphorylated TPS calibration standards for TPS substrate peptides in the *in vitro* kinase activity assay reaction mixture, thus subjecting them to all steps of sample incubation and preparation that potentially diminish their recovery. This calibration procedure compensated for the different phosphopeptide recoveries and therefore allowed absolute quantification of TPS phosphopeptides formed during *in vitro* incubations.

As can be seen in Fig. 5 and Table I, the multiparallel kinase activity assay in the presence of synthetic TPS peptides clearly discriminates among phosphorylation specificities, thus providing evidence for different kinase substrate affinities. (Such discrimination may be particularly useful for experiments involving multiple types of factors like time points,

treatments, and tissue types and for biological replicates.) TPS peptides 2, 12, 13, and 15 exhibit a proline residue at position −1 (adjacent to the target serine/threonine). Except for TPS peptide 15, which acted as a kinase target (formation of about 2 pmol of corresponding phospho-TPS peptide), the *in vitro* incubation of the other three TPS peptides yielded none or only very low amounts (below 0.5 pmol) of the phosphorylated counterparts (see Fig. 5 and Table I). The presence of a proline residue can significantly affect polypeptide structure with the result that sequences may be kinked or bent (48). Although TPS peptides 2 and 12 exhibit a preferred consensus motif designating them as rather good substrates, their phosphorylated analogues did not form. This might be due to the proline residue at −1, which, by producing kinks in these peptides, may impair kinase binding. Studies of target peptide variants are needed to identify the effect of this proline residue on substrate targeting.

TPS peptides 5, 6, 13, and 16 contain the less preferred consensus motif for SnRK1s (47). In contrast to the preferred consensus sequence where the requisite basic residue is located in position −3 with respect to the target serine/threonine, here the basic residue is in −4 (see Fig. 4). These peptides might therefore be suspected to make poor SnRK1 substrates. *In vitro* incubations revealed that kinases did not phosphorylate TPS peptides 5, 13, and 16 in either the presence or absence of Ca^{2+}. TPS peptide 6, on the other hand, was phosphorylated. However, the rather low phosphorylation level of this substrate peptide remains consistent with the presence of the less preferred consensus motif for SnRK1s.

The observation that phosphopeptide formation for six of the TPS substrate peptides is Ca^{2+}-dependent (Fig. 5 and Table I) implies that additional, Ca^{2+}-dependent kinases in the crude extract also recognize these peptides. In fact, the consensus sequence for SnRK1s includes the minimal recognition motif for calcium-dependent protein kinases (CDPKs), generally given as φ-*X*-Basic-*X*-*X*-Ser-*X*-*X*-*X*-φ where φ is a hydrophobic residue and *X* is any residue (15). That CDPKs and SnRK1s have similar recognition motifs is consistent with the fact that both protein kinases are members of the same family (12). The complete inhibition of the *in vitro* phosphorylation of TPS peptides 7, 11, and 15 by substitution of $CaCl_2$ with EGTA, however, excludes a role of SnRK1s in the phosphorylation of these peptides and strongly suggests the phosphorylation seen is exclusively the work of CDPKs. Interestingly all TPS peptides with *in vitro* phosphorylation not dependent on Ca^{2+} exhibit a target threonine instead of a serine.

Not only were differences in the degree of and the Ca^{2+} dependence of phosphorylation observed among various members of the TPS gene family, variation was also seen among TPS peptides originating from the same TPS isozymes. For example, TPS peptides 9, 10, 11, and 12, all representing TPS isozyme At1g60140, exhibited diverse behavior in the *in vitro* kinase assay. TPS peptide 10 was phosphorylated in a Ca^{2+}-independent manner, whereas the phosphorylation of TPS peptides 9 and 11 was Ca^{2+}-dependent. TPS peptide 12 did not act as a kinase substrate at all. TPS isozyme At1g68020 peptides 13, 14, and 15 showed little or no phosphorylation, offering this isozyme a potential function as a negative *in vitro* kinase activity control for future studies.

Besides their SnRK1/CDPK phosphorylation sites many TPS substrate peptides have additional serine and/or threonine residues in their sequence that are potential phosphorylation targets of other kinase families. Because the MRM approach used in this study is not suitable for the identification of the specific phosphorylation sites of the TPS phosphopeptides, MS^3 spectra from standard TPS phosphopeptides and phosphopeptides formed in the *in vitro* kinase activity assay were recorded using a linear ion trap mass spectrometer. MS^2 spectra generated from phosphopeptides often do not provide enough peptide backbone fragmentation necessary for unambiguous identification of phosphorylation sites because of a dominant neutral loss of phosphoric acid during MS^2 fragmentation (40). Here we made use of the neutral loss peak derived from serine/threonine phosphorylated TPS peptides to trigger a data-dependent MS^3 fragmentation step. However, a chromatographic separation of the *in vitro* phosphorylated TPS peptides in front of mass spectrometric analysis as described under "Experimental Procedures" is indispensable for good quality MS^3 spectra. This ensures that other compounds and contaminations present in the reaction mixture are clearly separated thus limiting unwanted ionization suppression by the matrix. The resulting neutral loss-driven MS^3 spectra of phosphorylated TPS peptides are informative enough to identify the correct phosphorylation site. It could be shown that the MS^3 spectra of the synthetic standard TPS phosphopeptides were identical to the MS^3 spectra generated from *in vitro* formed TPS phosphopeptides. Consequently an *in vitro* phosphorylation of alternative residues within the TPS peptide sequences could be ruled out. Fig. 6 exemplarily shows a comparison of full MS^3 spectra generated from standard phospho-TPS peptides 1, 3, 4, 6, and 15 (all containing additional serine/threonine residues in their sequences) and their counterparts formed *in vitro*.

With regard to the selectivity of detection the triple stage quadrupole instrument operated in MRM mode yielded significantly higher S/N ratios (up to 50-fold) for the TPS phosphopeptides than the linear ion trap mass spectrometer in the neutral loss-driven MS^3 scanning mode when using the same chromatographical conditions. Theoretically the neutral loss-driven MS^3 approach is more selective than MS^2-based MRM because of one additional fragmentation step in the detection method. However, the enhanced resolution achieved by the quadrupole mass filters of the triple stage quadrupole instrument compensates for that. The relatively low mass accuracy of ion trap instruments does not allow for highly specific precursor selection. As a result, the S/N of detection is greatly increased using the MRM-based approach. This is reflected

by the LODs for the TPS phosphopeptides that ranged from 20 fmol to 1.1 pmol for MRM detection (Table I), whereas the LODs using the neutral loss-driven MS^3 approach were estimated to be in the picomolar range.

In the near future, the comparison of wild-type and mutant plants harvested at different points of the day/night cycle will allow a deeper insight into the phosphoregulation of TPS. With the simultaneous analysis outlined here, it is possible to cross-correlate TPS isozyme phosphorylation data with quantitative expression data. The utilization of peptide libraries will enable the fast and simultaneous analysis of hundreds of peptides. Especially important is the use of peptides containing putative phosphorylation sites predicted by bioinformatic analysis of the proteome and prediction of consensus motifs (non-random peptide libraries) as demonstrated in this study. In this regard, the method has potential implications for the fast and robust testing of new peptide substrates to distinguish activities of CDPKs from those of SnRK1s (even in crude extracts) and for the screening of new phosphorylation sites in plant proteins.

Acknowledgments—We thank Nima Keshvari for deducing the target peptide sequences. Furthermore we thank Megan McKenzie for critical reading of the manuscript. Technical assistance of Stanislav Krüger is gratefully acknowledged.

* This work was supported by the Max Planck Society. The costs of publication of this article were defrayed in part by the payment of page charges. This article must therefore be hereby marked "*advertisement*" in accordance with 18 U.S.C. Section 1734 solely to indicate this fact.

‡ To whom correspondence should be addressed. Tel.: 49-331-5678109; Fax: 49-331-5678134; E-mail: weckwerth@mpimp-golm-mpg.de.

REFERENCES

1. Roessner, U., Wagner, C., Kopka, J., Trethewey, R. N., and Willmitzer, L. (2000) Technical advance: simultaneous analysis of metabolites in potato tuber by gas chromatography-mass spectrometry. *Plant J.* **23,** 131–142
2. Garcia, A. B., Engler, J., Iyer, S., Gerats, T., Van Montagu, M., and Caplan, A. B. (1997) Effects of osmoprotectants upon NaCl stress in rice. *Plant Physiol.* **115,** 159–169
3. Vogel, G., Fiehn, O., Jean-Richard-dit-Bressel, L., Boller, T., Wiemken, A., Aeschbacher, R. A., and Wingler, A. (2001) Trehalose metabolism in Arabidopsis: occurrence of trehalose and molecular cloning and characterization of trehalose-6-phosphate synthase homologues. *J. Exp. Bot.* **52,** 1817–1826
4. Adams, R. P., Kendall, E., and Kartha, K. K. (1990) Comparison of free sugars in growing desiccated plants of Selaginella-Lepidophylla. *Biochem. Syst. Ecol.* **18,** 107–110
5. Gomez, L. D., Baud, S., and Graham, I. A. (2005) The role of trehalose-6-phosphate synthase in Arabidopsis embryo development. *Biochem. Soc. Trans.* **33,** 280–282
6. van Dijken, A. J., Schluepmann, H., and Smeekens, S. C. (2004) Arabidopsis trehalose-6-phosphate synthase 1 is essential for normal vegetative growth and transition to flowering. *Plant Physiol.* **135,** 969–977
7. Schluepmann, H., van Dijken, A., Aghdasi, M., Wobbes, B., Paul, M., and Smeekens, S. (2004) Trehalose mediated growth inhibition of Arabidopsis seedlings is due to trehalose-6-phosphate accumulation. *Plant Physiol.* **135,** 879–890
8. Eastmond, P. J., Li, Y., and Graham, I. A. (2003) Is trehalose-6-phosphate a regulator of sugar metabolism in plants? *J. Exp. Bot.* **54,** 533–537
9. Thimm, O., Blasing, O., Gibon, Y., Nagel, A., Meyer, S., Kruger, P., Selbig, J., Muller, L. A., Rhee, S. Y., and Stitt, M. (2004) MAPMAN: a user-driven tool to display genomics data sets onto diagrams of metabolic pathways and other biological processes. *Plant J.* **37,** 914–939
10. Leonhardt, N., Kwak, J. M., Robert, N., Waner, D., Leonhardt, G., and Schroeder, J. I. (2004) Microarray expression analyses of Arabidopsis guard cells and isolation of a recessive abscisic acid hypersensitive protein phosphatase 2C mutant. *Plant Cell* **16,** 596–615
11. Eastmond, P. J., van Dijken, A. J., Spielman, M., Kerr, A., Tissier, A. F., Dickinson, H. G., Jones, J. D., Smeekens, S. C., and Graham, I. A. (2002) Trehalose-6-phosphate synthase 1, which catalyses the first step in trehalose synthesis, is essential for Arabidopsis embryo maturation. *Plant J.* **29,** 225–235
12. Hrabak, E. M., Chan, C. W., Gribskov, M., Harper, J. F., Choi, J. H., Halford, N., Kudla, J., Luan, S., Nimmo, H. G., Sussman, M. R., Thomas, M., Walker-Simmons, K., Zhu, J. K., and Harmon, A. C. (2003) The Arabidopsis CDPK-SnRK superfamily of protein kinases. *Plant Physiol.* **132,** 666–680
13. Bhalerao, R. P., Salchert, K., Bako, L., Okresz, L., Szabados, L., Muranaka, T., Machida, Y., Schell, J., and Koncz, C. (1999) Regulatory interaction of PRL1 WD protein with Arabidopsis SNF1-like protein kinases. *Proc. Natl. Acad. Sci. U. S. A.* **96,** 5322–5327
14. McMichael, R. W., Jr., Bachmann, M., and Huber, S. C. (1995) Spinach leaf sucrose-phosphate synthase and nitrate reductase are phosphorylated/inactivated by multiple protein kinases in vitro. *Plant Physiol.* **108,** 1077–1082
15. Bachmann, M., Shiraishi, N., Campbell, W. H., Yoo, B. C., Harmon, A. C., and Huber, S. C. (1996) Identification of Ser-543 as the major regulatory phosphorylation site in spinach leaf nitrate reductase. *Plant Cell* **8,** 505–517
16. Toroser, D., McMichael, R., Krause, K. P., Kurreck, J., Sonnewald, U., Stitt, M., and Huber, S. C. (1999) Site-directed mutagenesis of serine 158 demonstrates its role in spinach leaf sucrose-phosphate synthase modulation. *Plant J.* **17,** 407–413
17. Hardin, S. C., Winter, H., and Huber, S. C. (2004) Phosphorylation of the amino terminus of maize sucrose synthase in relation to membrane association and enzyme activity. *Plant Physiol.* **134,** 1427–1438
18. Moorhead, G., Douglas, P., Cotelle, V., Harthill, J., Morrice, N., Meek, S., Deiting, U., Stitt, M., Scarabel, M., Aitken, A., and MacKintosh, C. (1999) Phosphorylation-dependent interactions between enzymes of plant metabolism and 14-3-3 proteins. *Plant J.* **18,** 1–12
19. Romeis, T., Ludwig, A. A., Martin, R., and Jones, J. D. G. (2001) Calcium-dependent protein kinases play an essential role in a plant defence response. *EMBO J.* **20,** 5556–5567
20. Romeis, T. (2001) Protein kinases in the plant defence response. *Curr. Opin. Plant Biol.* **4,** 407–414
21. Laurie, S., and Halford, N. G. (2001) The role of protein kinases in the regulation of plant growth and development. *Plant Growth Regul.* **34,** 253–265
22. MacKintosh, C. (1998) Regulation of cytosolic enzymes in primary metabolism by reversible protein phosphorylation. *Curr. Opin. Plant Biol.* **1,** 224–229
23. Toroser, D., and Huber, S. C. (1997) Protein phosphorylation as a mechanism for osmotic-stress activation of sucrose-phosphate synthase in spinach leaves. *Plant Physiol.* **114,** 947–955
24. Shao, J., and Harmon, A. C. (2003) In vivo phosphorylation of a recombinant peptide substrate of CDPK suggests involvement of CDPK in plant stress responses. *Plant Mol. Biol.* **53,** 691–700
25. Hubbard, M. J., and Cohen, P. (1993) On target with a new mechanism for the regulation of protein phosphorylation. *Trends Biochem. Sci.* **18,** 172–177
26. Cohen, P. (2000) The regulation of protein function by multisite phosphorylation—a 25 year update. *Trends Biochem. Sci.* **25,** 596–601
27. Zolnierowicz, S., and Bollen, M. (2000) Protein phosphorylation and protein phosphatases. De Panne, Belgium, September 19–24, 1999. *EMBO J.* **19,** 483–488
28. Kerk, D., Bulgrien, J., Smith, D. W., Barsam, B., Veretnik, S., and Gribskov, M. (2002) The complement of protein phosphatase catalytic subunits encoded in the genome of Arabidopsis. *Plant Physiol.* **129,** 908–925
29. Initiative, T. A. (2000) Analysis of the genome sequence of the flowering plant Arabidopsis thaliana. *Nature* **408,** 796–815
30. Sugden, C., Donaghy, P. G., Halford, N. G., and Hardie, D. G. (1999) Two

SNF1-related protein kinases from spinach leaf phosphorylate and inactivate 3-hydroxy-3-methylglutaryl-coenzyme A reductase, nitrate reductase, and sucrose phosphate synthase *in vitro*. *Plant Physiol.* **120,** 257–274
31. Douglas, P., Pigaglio, E., Ferrer, A., Halfords, N. G., and MacKintosh, C. (1997) Three spinach leaf nitrate reductase-3-hydroxy-3-methylglutaryl-CoA reductase kinases that are required by reversible phosphorylation and/or Ca^{2+} ions. *Biochem. J.* **325,** 101–109
32. Huber, S. C., and Huber, J. L. (1996) Role and regulation of sucrose-phosphate synthase in higher plants. *Annu. Rev. Plant Physiol. Plant Mol. Biol.* **47,** 431–444
33. Thelander, M., Olsson, T., and Ronne, H. (2004) Snf1-related protein kinase 1 is needed for growth in a normal day-night light cycle. *EMBO J.* **23,** 1900–1910
34. Zhang, Y., Shewry, P. R., Jones, H., Barcelo, P., Lazzeri, P. A., and Halford, N. G. (2001) Expression of antisense SnRK1 protein kinase sequence causes abnormal pollen development and male sterility in transgenic barley. *Plant J.* **28,** 431–441
35. Halford, N. G., Hey, S., Jhurreea, D., Laurie, S., McKibbin, R. S., Paul, M., and Zhang, Y. (2003) Metabolic signalling and carbon partitioning: role of Snf1-related (SnRK1) protein kinase. *J. Exp. Bot.* **54,** 467–475
36. Toroser, D., Plaut, Z., and Huber, S. C. (2000) Regulation of a plant SNF1-related protein kinase by glucose-6-phosphate. *Plant Physiol.* **123,** 403–412
37. Annan, R. S., and Carr, S. A. (1997) The essential role of mass spectrometry in characterizing protein structure: mapping posttranslational modifications. *J. Protein Chem.* **16,** 391–402
38. Neubauer, G., and Mann, M. (1999) Mapping of phosphorylation sites of gel-isolated proteins by nanoelectrospray tandem mass spectrometry: potentials and limitations. *Anal. Chem.* **71,** 235–242
39. Steen, H., Kuster, B., and Mann, M. (2001) Quadrupole time-of-flight versus triple-quadrupole mass spectrometry for the determination of phosphopeptides by precursor ion scanning. *J. Mass Spectrom.* **36,** 782–790
40. Schlosser, A., Pipkorn, R., Bossemeyer, D., and Lehmann, W. D. (2001) Analysis of protein phosphorylation by a combination of elastase digestion and neutral loss tandem mass spectrometry. *Anal. Chem.* **73,** 170–176
41. DeGnore, J. P., and Qin, J. (1998) Fragmentation of phosphopeptides in an ion trap mass spectrometer. *J. Am. Soc. Mass Spectrom.* **9,** 1175–1188
42. Glinski, M., Romeis, T., Witte, C. P., Wienkoop, S., and Weckwerth, W. (2003) Stable isotope labeling of phosphopeptides for multiparallel kinase target analysis and identification of phosphorylation sites. *Rapid Commun. Mass Spectrom.* **17,** 1579–1584
43. Mann, M., Ong, S. E., Gronborg, M., Steen, H., Jensen, O. N., and Pandey, A. (2002) Analysis of protein phosphorylation using mass spectrometry: deciphering the phosphoproteome. *Trends Biotechnol.* **20,** 261–268
44. Kratzer, R., Eckerskorn, C., Karas, M., and Lottspeich, F. (1998) Suppression effects in enzymatic peptide ladder sequencing using ultraviolet-matrix assisted laser desorption/ionization-mass spectrometry. *Electrophoresis* **19,** 1910–1919
45. Bradford, M. M. (1976) Rapid and sensitive method for quantitation of microgram quantities of protein utilizing principle of protein-dye binding. *Anal. Biochem.* **72,** 248–254
46. Matuszewski, B. K., Constanzer, M. L., and Chavez-Eng, C. M. (2003) Strategies for the assessment of matrix effect in quantitative bioanalytical methods based on HPLC-MS/MS. *Anal. Chem.* **75,** 3019–3030
47. Halford, N. G., and Hardie, D. G. (1998) SNF1-related protein kinases: global regulators of carbon metabolism in plants? *Plant Mol. Biol.* **37,** 735–748
48. Kang, Y. K., Jhon, J. S., and Han, S. J. (1999) Conformational study of Ac-Xaa-Pro-NHMe dipeptides: proline puckering and trans/cis imide bond. *J. Pept. Res.* **53,** 30–40